Title: Peculiar properties of phase transitions in Na0.5Bi0.5TiO3-xBaTiO3 (0<x<6) lead-free relaxor ferroelectrics seen via acoustic emission

Author: Eveniy Dul'kin, Jan Suchanicz, Antoni Kania, Michael Rotha

Peculiar Properties of Phase Transitions in $Na_{0.5}Bi_{0.5}TiO_3$-$xBaTiO_3$ (0<x<6) Lead-free Relaxor Ferroelectrics Seen Via Acoustic Emission

Eveniy Dul'kin[a]*, Jan Suchanicz[b], Antoni Kania[c], Michael Roth[a]

[a]Department of Applied Physics, The Hebrew University of Jerusalem, Jerusalem 91904, Israel
[b]Institute of Technology, Pedagogical University, Krakov 30-084, Poland
[c]A.Chelkowski Institute of Physics, University of Silesia, Uniwersytecka 4, 40-007 Katowice, Poland

$Na_{0.5}Bi_{0.5}TiO_3$-$xBaTiO_3$ (0<x<6) relaxor ferroelectrics crystals were investigated by means of dielectric and acoustic emission methods. Dielectric curves exhibit the slightly visible small maxima near the depolarization temperatures, T_d, and the wide maxima at the temperatures of T_m, whereas the acoustic emission exhibits the sharp bursts, corresponding to T_d, T_{lm}, which is known to be a temperature exhibiting a strong frequency dispersion, T_{RE}, which is known to be a temperature above which a frequency dispersion vanishes, and the T_m and the T_p manifesting a transition to the paraelectric phase. Based on the AE data it was established that all these characteristic temperatures shift down as x increases, but with different slopes. A mechanism of such the differences is discussed.

Keywords: *Relaxor ferroelectrics, phase transformations, depolarization temperature, Curie temperature, acoustic emission.*

1. Introduction

Relaxor ferroelectrics (RFEs) include a large group of solid solutions and complex compounds (mostly oxides) with ABO_3 perovskite structure, and their properties are known to be in contrast to the ordered ferroelectrics (FEs). Both Pb-based and Pb-free $A(B'_{1/2}B''_{1/2})O_3$ and $A(B'_{1/3}B''_{2/3})O_3$ relaxors attract a great attention due to their intrinsic chemical inhomogeneity and related local structural distortions due to the difference in ionic charges and radii between the different kinds of B- or A-site cations in the former (Pb-based)[1], or on both A- and B-sites in the latter (Pb-free compounds)[2], which is a reason of the existence of polar nanoregions (PNRs) resulting in the giant and smeared maxima of dielectric permittivity, ε', at temperature referred as T_m, which depends on the measuring frequency. Being mobile the PNRs nucleate at high enough Burns temperature, T_B, on cooling, below so-called intermediate temperature, T^*, they begin to couple and merge into larger ones, become a long-lived and so the deviation from a Curie-Weiss law and a frequency dispersion starts[3], and on further cooling the PNRs become frozen into a nonergodic dipole glass state below Vogel-Fulcher temperature, ascribed as freezing temperature, T_f, some degrees below the T_m[1-3]. While all these characteristic points: T_B, T^* and T_m, were detected in Pb-based RFEs[4-7] as well as in some Pb-free RFEs[8,9], in Pb-free relaxors of $Na_{0.5}Bi_{0.5}TiO_3$-$xBaTiO_3$ (NBT-xBT) they have been established recently using an acoustic emission (AE) method[10]. Moreover, in the latter paper it was shown

that the temperature T_{lm}, corresponding to local dielectric maxima of ε', or so-called "hump", low temperature and frequency dependent one, plays a role of T_m in the Pb-based RFEs and is caused by interaction between PNRs only, whereas the high temperature maximum of ε', ascribed as to be corresponding to T_m, is caused of coexisting of some phases with which NBT-xBT is known to be rich.

In accordance with the structural studies a sequence of the phase transitions when heating the pure unpoled NBT crystals and ceramics is following: Trigonal I FE → Trigonal II Antiferroelectrics (AFE) → Tetragonal Ferroelastic (FEl)→ Cubic Paraelectric (PE) at 200, 320 and 547°C with coexisting Trigonal II and Tetragonal phases through 277 ÷ 367°C[11], Rhombohedral FE $R3c$ → Tetragonal AFE $P4bm$ → Cubic PE $Pm\overline{3}m$ at 255, 400 and 540°C with coexisting $R3c$ and $P4bm$ through 255 ÷ 400°C and $P4bm$ and $Pm\overline{3}m$ through 500 ÷ 540°C[12], FE → AFE → FEl → PE at 200, 320 and 540°C[13]. While the high-temperature data of two latter works coincides well, the data of former work is inconsistent with them due to presence of low-temperature Trigonal I → Trigonal II phase transition near 200°C[11]. Later it was shown[12], that there is not any phase transition between room temperature and 250°C, and the observed steep drop of piezomodulus higher than the so-called depolarization temperature, $T_d \approx$ 190°C[14], is presumably caused by percolation of disordered $P4bm$ nano-scale platelets[15], embedded in the $R3c$ matrix in pure NBT[16].

Along with the piezomodulus, on heating the dielectric constant exhibits anomalies around of 200°C, slightly above T_d[17-21], accompanied by strong frequency dispersion as well as marks out the AFE *P4bm* to PE *Pm$\overline{3}$m* phase transition around the T_m of 320°C[17-21]. Also these two dielectric anomalies usually accompanied by jumps of the thermal expansion coefficient[17], peaks of differential scanning calorimetry curve[22], electrostrictive strain[23] and elastic compliance[24]. In addition, on heating the domain twins appear near 260°C and disappear near 295°C, whereas on cooling they appear near 240°C and disappear near 205°C, exhibiting a hysteresis of about 55°C[22,25] and disappear above approximately 540°C[25,26].

When incorporating the Ba ions in A-site of NBT-*x*BT the dielectric anomalies smear and shift by the temperature, but the direction of such the shifts is not clearly seen due to smearing of dielectric curves as well as contradictory sometimes, especially concerning the T_m[19-21,27-29]. Moreover, in pure NBT the maximum of ε' there is a clearly seen to be not symmetric: jump of ε' on some tens of degrees below T_m, shifting to lower temperatures and gradually vanishing as the content of Ba increases[20,21]. Note, that this jump of ε' approximately coincides with disappearance of the domain twins near 295°C[22,25].

Scrupulous observations of domain morphology, performed with NBT-*x*BT, allowed the authors[30-32] to establish an existence of two-phase mixture (complex domains) with volumes of *R3c* FE domains (~100nm) embedded in the matrix of *P4bm* AFE nanodomains (<20nm), PNRs, in NBT-6BT ceramics (core-shell grain structure) at room temperature, that does provide the excellent piezoelectric properties. In particularly, in NBT-6BT particularly, lying in the middle of morphotropic phase boundary, around 40% of the grains display such complex domains with *R3c-P4bm* structure, while the rest ones display *P4bm* PNRs only. On heating the volume fraction, containing these complex FE domains, starts to shrink at around $T_d \approx 120$°C and this process continues until ~160°C when the whole grain is completely occupied by PNRs with *P4bm* symmetry. The $R3c \rightarrow P4bm$ structural phase transition undergoes through the finite temperature interval of about 40°C: the volume with *P4bm* PNRs expands at the expense of the volume with the *R3c* complex domains and finally occupies the whole grain. During further heating the major part of *P4bm* PNRs transform to *P4bm* long-range phase near $T_{RE} \approx 220$-230°C though their small amount exists far above the T_m[32], and above of 335°C the tetragonal - cubic structural phase transition takes place at T_p.

Previously the dielectric constant, measured on heating in NBT-6BT crystals, clearly shows the low temperature "hump" of ε'[19,27-30] between of 140 and 220°C, accompanied by AE bursts between of 127 and 225°C, which also exhibits the bursts corresponding to $T_m \approx 290$°C and $T_p \approx 390$°C,

respectively[33]. Recently, using the AE, it was confirmed that the temperature of this "hump", ascribed as the T_{lm}, exhibits the strong frequency dispersion, whereas the T_d exhibits no dispersion, and all these characteristic temperatures of NBT-6BT: $T_d \approx 123$°C, $T_{lm} \approx 150 \div 180$°C, $T_{RE} \approx 225$°C, $T_m \approx 300 \div 310$°C and $T_p \approx 327$°C have been successfully detected by AE[10], in good agreement with the early detected data[33].

Because AE has proven itself to be a reliable method to detect all the characteristic temperatures in NBT-6BT relaxors ferroelectrics more precisely in comparing with the smeared maximum of dielectric permittivity, we have applied it to detect of these temperatures in NBT-*x*BT compounds and to study their shift in dependence on the Ba content.

2. Experimental Details

Na$_{0.5}$Bi$_{0.5}$TiO$_3$-*x*BaTiO$_3$ (*x* = 0; 2; 2,5; 3,25 and 6) crystals were grown using a Czochralski method. Powder reagents of Na$_2$CO$_3$, BaCO$_3$, Bi$_2$O$_3$ and TiO$_2$ were used as the starting materials. Stoichiometric amounts were weighed and homogenized in agate vessel in alcohol for 2 h. The obtained mixture was then calcined at 800ºC for 4 h. The crystal growths were carried out at concentration dependent temperatures from the range 1300-1360ºC. The obtained crystals with dimensions about 1.5 mm × 1.5 mm × 2.5 mm were homogeneous, transparent and slightly yellowish. No cracks and inclusions were observed. The silver contacts were fired at 650°C for 30 min. We used the unpoled samples in order to avoid the changing in phase structure that can be completely altered after applying an electric field[17].

AE is known to be a nondestructive method, based on detection of the mechanical elastic waves, radiated by the different structural defects in the solid states under some external loadings: stress, temperature, electric field, as well as by arising of the mechanical twins during the martensite phase transitions in metals and their alloys. The waves are detected using a piezoelectric sensor, fairly often connected with the sample through a dielectric acoustic waveguide to avoid of its overheating[34]. Traditionally in FEs the AE is well proven in detection of the structural phase transitions, T_c, due to arising of the domains and their mechanical interaction[35-38] as well as recently it is well proven in a study of all the characteristic temperatures in RFEs: T_m, T^* and T_B due to arising of the PNRs and their mechanical interaction[4-10,33].

AE technique has been described previously elsewhere[11]. A sample was pasted with a silver epoxy on the polished side of a fused silica acoustic rod waveguide. A PZT-19 disk piezoelectric sensor was attached to the rear end of the waveguide. A sensor was electrically coupled to a 500 kHz bandpass low noise variable (up to 40 dB) preamplifier connected to a detector-amplifier (40 dB). A Ch-Al thermocouple junction was glued to the waveguide near the sample. A

Peculiar Properties of Phase Transitions in Na$_{0.5}$Bi$_{0.5}$TiO$_3$-xBaTiO$_3$ (0<x<6) Lead-free Relaxor Ferroelectrics
Seen Via Acoustic Emission

3

waveguide with the pasted sample is vertically mounted from below into resistance element furnace. The dielectric data were measured using a HP4263A LCR meter wired to the sample. All the thermocouple, amplifier, and LCR meter outputs were interfaced with a PC for a coupled readout. The measurement of the dielectric constant real part ε' and AE count rate $\dot{N}$ (s^{-1}) were performed in the temperature range of 20-400°C with a rate of about 1-3°C/min at the measuring frequency of 1 kHz on heating.

3. Result and Discussion

Figure 1 presents the temperature dependences of the real part of dielectric constant ε' and AE count rate $\dot{N}$ for all the compounds. The $\varepsilon'(T)$ curves exhibit two groups of smeared (diffused) humps and maxima: the low temperature humps corresponds to T_{lm}, in the range of 150-200°C and the high temperature maxima corresponds to T_m in the range of 300-350°C. These results are in good agreement with previous studies[10,19,21,27-31,33]. For pure NBT the form of the ε' curve is not symmetric around T_m: from the low temperature side it is steeper in comparison with the high temperature side, as observed previously[21]. With an increase in the Ba content the dielectric constant ε' around T_m becomes symmetric and gradually rises in both the T_d and T_m when they shift towards the lower temperature in good coincidence with the previously observed data, too[19,20,22].

AE exhibits four bursts in all the compounds, corresponding to $T_d \approx 105$ °C ($\dot{N} \approx 30$ s^{-1}), 112 °C ($\dot{N} \approx 40$ s^{-1}), 116 °C ($\dot{N} \approx 45$ s^{-1}), 123 °C ($\dot{N} \approx 50$ s^{-1}), 130°C ($\dot{N} \approx 34$ s^{-1}); $T_{lm} \approx 160$°C ($\dot{N} \approx 30$ s^{-1}), 175°C ($\dot{N} \approx 30$ s^{-1}), 180°C ($\dot{N} \approx 20$ s^{-1}), 188°C ($\dot{N} \approx 30$ s^{-1}), 200°C ($\dot{N} \approx 40$ s^{-1}); $T_{RE} \approx 230$°C ($\dot{N} \approx 20$ s^{-1}), 275°C ($\dot{N} \approx 24$ s^{-1}), 285°C ($\dot{N} \approx 20$ s^{-1}), 300°C ($\dot{N} \approx 24$ s^{-1}), 331°C ($\dot{N} \approx 20$ s^{-1}); $T_m \approx 298$°C ($\dot{N} \approx 50$ s^{-1}), 315°C ($\dot{N} \approx 40$ s^{-1}), 322°C ($\dot{N} \approx 36$ s^{-1}), 333°C ($\dot{N} \approx 50$ s^{-1}), 342°C ($\dot{N} \approx 34$ s^{-1}), except of NBT-6BT, in which it exhibits the sixth burst, corresponding to $T_p \approx 330$°C ($\dot{N} \approx 70$ s^{-1}). Two lowest bursts clearly separate the T_d, exhibiting no frequency dispersion, from T_{lm}, exhibiting the essential frequency dispersion[10,18-20,27] and obeying the Vogel-Fulcher law[39]. For pure NBT both the T_{RE} and T_m are located close to each other what causes the non symmetric form of ε' curve around T_m.

Although the AE bursts exhibits some scattering in the values, some trends of $\dot{N}$ distribution are still visible (Table 1). Indeed, it is well seen that the values of $\dot{N}$, corresponding to both T_d and T_m, are stronger than the one, corresponding to T_{RE}. Such the distribution of values of $\dot{N}$ is similar that previously observed when transforming through the $R3m$ rhombohedral - $Amm2$ orthorhombic - $P4mm$ tetragonal - $Pm\overline{3}m$ cubic phase transitions in BaTiO$_3$ ceramics[35]. Moreover, it is clearly seen, too, that the $\dot{N}$ becomes stronger when transforming through the AFE $P4bm$ - FEl $P4/mbm$ - PE

$Pm\overline{3}m$ phases in good coincides with one previously observed in some well-known perovskite FEs, undergoing through the AFE - FE - PE phases[37]. Thus, one can conclude the AE method rightly reflects the sequence of the phase transitions in RFEs and so could be to apply for express identification of their phase transitions types by the quantities of $\dot{N}$, as it was revealed in Ref.[37].

All the AE bursts point out the phase transitions, taking place in NBT-xBT compounds, except of T_{lm}. AE bursts, accompanying the T_{lm} was recently shown to correspond the interaction between the PNRs only[10]. Concerning the phase transitions they can be qualified based on the structural data[11-16] and scrupulous studies of domain structure[22,25,26,30-32]. On heating at T_d the $R3c \rightarrow P4bm$ phase transition starts and this temperature is even ascribed to be the Curie temperature, T_c[26], and such the statement closes a row of the characteristic points in NBT-xBT family: $T_d \equiv T_c$, $T_{lm} \equiv T_m$ of Pb-based RFEs, $T_{RE} \equiv T^{*}$[10], and the $T_B \approx 420 \div 450$°C[40]. During this phase transition the frequency dispersion of a dielectric constant exists up to T_{RE}, where the long-range $P4bm$ phase arises. So, the relaxor property of NBT-xBT continues from T_d to T_{RE}. Presumably, at T_m the $P4bm$ phase transforms to the tetragonal centrosymmetric $P4/mbm$ nonpolar ferroelastic phase[16], which further transforms to $Pm\overline{3}m$ phase at T_p. AE points out the $T_p \approx 330$°C only for NBT-6BT compound, for other compositions the T_p lies upper of a heating possibility of our furnace.

Figure 2 presents the temperatures of all the characteristic points, detected by AE, as a function of Ba content x. All the temperatures decrease linearly with ecreasing x. Similar linear down of T_c was earlier observed in BaTiO$_3$ crystals when substituting the Ba ion by its heavier isotope[41]. So, a decrease in the phase transitions temperatures with enhancement of x leads us to conclude that the Ba ion mainly substitutes the light Na ion rather than the heavy Bi ion, especially since both radii of Na and Bi are nearly equal to each other: 1.18Å ≈ 1.17Å (CN = 8).

On the other hand, the slopes of these linear dependencies are essentially different. Indeed, while the slopes of T_m, T_{lm} and T_d are found to be approximately the same order of magnitude: -7.3, -6.6, and -4.2, respectively, the slope of T_{RE} is found to be -16,6 as well. Taking into account that both the FE $R3c$ and AFE $P4bm$ phases coexist between T_d and T_{RE}, we tend to think that such the steep slope of the $T_{RE}(x)$ dependence is caused by a chemical pressure contributed by the incorporated Ba ions as their content increases. Recently based on both the theoretical and experimental data it was shown that a pressure downs the temperature of FE-AFE phase transition steeper than the temperature of AFE-PE phase transition[42], in good agreement with our present data. And, thus, we have confirmed that $P4bm$ phase is really the AFE one.
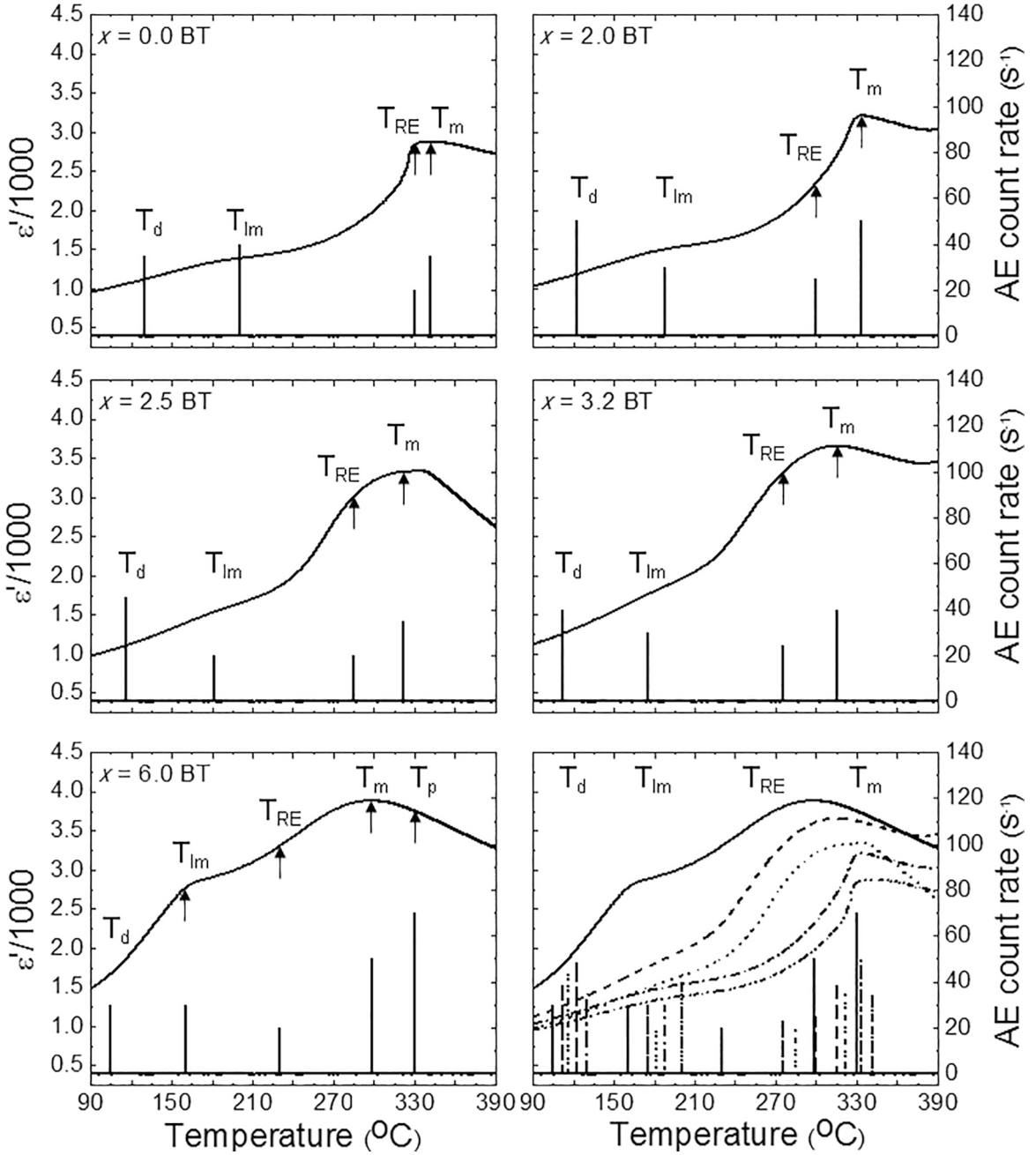
Figure 1. The plot of dielectric and acoustic emission data measured in $Na_{0.5}Bi_{0.5}TiO_3$-xBaTiO$_3$ relaxor ferroelectrics crystals (dash-dot-dot: x=0.00; dash-dot: x=0.02; dot: x=0.025; dash: x=0.0325; solid: x=0.06).

Table 1. Values of AE count rate $\dot{N}$, corresponding to T_d, T_{lm}, T_{RE}, T_m and T_p in NBT-xBT crystals.

	$\dot{N}$ (s⁻¹)				
	x = 0.0	x = 2.0	x = 2.5	x = 3.2	x = 6.0
T_d	34	50	45	40	30
T_{lm}	40	30	20	30	30
T_{RE}	20	24	20	24	20
T_m	34	50	36	40	50
T_p					70

Peculiar Properties of Phase Transitions in Na$_{0.5}$Bi$_{0.5}$TiO$_3$-xBaTiO$_3$ (0<x<6) Lead-free Relaxor Ferroelectrics
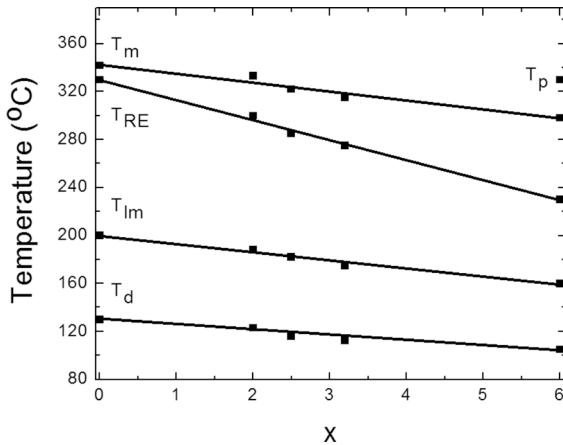Seen Via Acoustic Emission

5

Figure 2. The plot of downs the phase transitions temperatures detected by acoustic emission in Na$_{0.5}$Bi$_{0.5}$TiO$_3$-xBaTiO$_3$ relaxor ferroelectrics crystals in dependence on x.

4. Conclusion

In summary, we have investigated the Na$_{0.5}$Bi$_{0.5}$TiO$_3$-xBaTiO$_3$ (0<x<6) relaxor ferroelectrics crystals by means of dielectric and acoustic emission methods. We have detected all the phase transitions: ferroelectric-rhombohedral →antiferroelectric-tetragonal, starting above T_d and finishing above T_{RE}; antiferroelectric-tetragonal → ferroelastic-tetragonal at T_m; and ferroelastic-tetragonal → paraelectric-cubic at T_p. We have plotted the shifts of these temperatures with dependence on Ba content and established that all the temperatures decrease as Ba content increases. Also we have found out that the T_{RE} decreases steeper in comparing with the others and have shown that such the steeper decrease of T_{RE} is characterisitc for ferroelectric-rhombohedral → antiferroelectric-tetragonal phase transition when enhancing an intrinsic pressure as Ba content increases.

5. References

1. Bokov AA, Ye ZG. Recent progress in relaxor ferroelectrics with perovskite structure. *Journal of Materials Science*. 2006;41(1):31-52.

2. Shvartsman VV, Lupascu DC. Lead-Free Relaxor Ferroelectrics. *Journal of the American Ceramic Society*. 2012;95(1):1-26.

3. Toulouse J. The Three Characteristic Temperatures of Relaxor Dynamics and Their Meaning. *Ferroelectrics*. 2008;369(1):203-213.

4. Dul'kin E, Roth M, Janolin PE, Dkhil B. Acoustic emission study of phase transitions and polar nanoregions in relaxor-based systems: Application to the PbZn$_{1/3}$Nb$_{2/3}$O$_3$ family of single crystals. *Physical Review B*. 2006;73(1):012102.

5. Dkhil B, Gemeiner P, Al-Barakaty A, Bellaiche L, Dul'kin E, Mojaev E, et al. Intermediate temperature scale T* in lead-based relaxor systems. *Physical Review B*. 2009;80(6):064103.

6. Dul'kin E, Mihailova B, Gospodinov M, Roth M. Effect of A-site La, Ba, and Sr doping on the threshold field and characteristic temperatures of PbSc$_{0.5}$Nb$_{0.5}$O$_3$ relaxor studied by acoustic emission. *Journal of Applied Physics*. 2013;113(5):054105.

7. Dul'kin E, Kania A, Roth M. Characteristic temperatures of PbFe$_{1/2}$Nb$_{1/2}$O$_3$ ferroelectrics crystals seen via acoustic emission. *Materials Research Express*. 2014;1(1):016105.

8. Dul'kin E, Zhai J, Roth M. Acoustic emission pronounced field-induced response near critical point in Ba$_{0.6}$Sr$_{0.4}$TiO$_3$ ferroelectrics. *Physica Status Solidi A*. 2014;211(7):1539-1544.

9. Dul'kin E, Kojima S, Roth M. Dielectric maximum temperature non-monotonic behavior in uniaxial Sr$_{0.75}$Ba$_{0.25}$Nb$_2$O$_6$ relaxor seen via acoustic emission. *Journal of Applied Physics*. 2011;110(4):044106.

10. Dul'kin E, Tiagunova J, Mojaev E, Roth M. Peculiar properties of phase transitions in Na$_{0.5}$Bi$_{0.5}$TiO$_3$-0.06BaTiO$_3$ lead-free relaxor ferroelectrics seen via acoustic emission. *Functional Material Letters*. 2017;10:1750048.

11. Siny IG, Tu CS, Schmidt VH. Critical acoustic behavior of the relaxor ferroelectric Na$_{1/2}$Bi$_{1/2}$TiO$_3$ in the intertransition region. *Physical Review B*. 1995;51(9):5659-5665.

12. Jones GO, Thomas PA. Investigation of the structure and phase transitions in the novel A-site substituted distorted perovskite compound Na$_{0.5}$Bi$_{0.5}$TiO$_3$. *Acta Crystallographica Section B*. 2002;58:168-178.

13. Isupov VA. Ferroelectric Na$_{0.5}$Bi$_{0.5}$TiO$_3$ and K$_{0.5}$Bi$_{0.5}$TiO$_3$ Perovskites and Their Solid Solutions. *Ferroelectrics*. 2005;315(1):123-147.

14. Hiruma Y, Nagata H, Takenaka T. Thermal depoling process and piezoelectric properties of bismuth sodium titanate ceramics. *Journal of Applied Physics*. 2009;105(8):084112.

15. Aksel E, Forrester JS, Kowalski B, Jones JL, Thomas PA. Phase transition sequence in sodium bismuth titanate observed using high-resolution x-ray diffraction. *Applied Physics Letters*. 2011;99(22):222901.

16. Trolliard G, Dorcet V. Reinvestigation of Phase Transitions in Na$_{0.5}$Bi$_{0.5}$TiO$_3$ by TEM. Part II: Second Order Orthorhombic to Tetragonal Phase Transition. *Chemistry of Materials*. 2008;20(15):5074-5082.

17. Smolenskii GA, Isupov VA, Agranovskaya AI, Krainik NN. New ferroelectrics of complex composition. *Soviet Physics Solid State*. 1961;2(11):2651-2654.

18. Tu CS, Siny IG, Schmidt VH. Sequence of dielectric anomalies and high-temperature relaxation behavior in Na$_{1/2}$Bi$_{1/2}$TiO$_3$. *Physical Review B*. 1994;49(17):11550-11559.

19. Xu C, Lin D, Kwok KW. Structure, electrical properties and depolarization temperature of (Bi$_{0.5}$Na$_{0.5}$)TiO$_3$-BaTiO$_3$ lead-free piezoelectric ceramics. *Solid State Science*. 2008;10(7):934-940.

20. Chen M, Xu Q, Kim BH, Ahn BK, Ko JH, Kang WJ, et al. Structure and electrical properties of (Na$_{0.5}$Bi$_{0.5}$)$_{1-x}$Ba$_x$TiO$_3$ piezoelectric ceramics. *Journal of the European Ceramic Society*. 2008;28(4):843-849.

21. Suchanicz J, Kruzina TV, Pozdeev VG, Popov SA. Influence of Ba addition on the dielectric and optic properties of (1-*x*) Na$_{0.5}$Bi$_{0.5}$TiO$_3$-*x*BaTiO$_3$ (x = 0, 0.025, 0.0325 and 0.05) single crystals. *Phase Transitions*. 2016;89(3):310-316.

22. Pronin IP, Syrnikov PP, Isupov VA, Egorov VM, Zaitseva NV. Peculiarities of phase transitions in sodium-bismuth titanate. *Ferroelectrics*. 1980;25(1):395-397.

23. Suchanicz J, Roleder K, Kania A, Hańaderek J. Electrostrictive strain and pyroeffect in the region of phase coexistence in Na$_{0.5}$Bi$_{0.5}$TiO$_3$. *Ferroelectrics*. 1988;77(1):107-110.

24. Cordero F, Craciun F, Trequattrini F, Mercadelli E, Galassi C. Phase transitions and phase diagram of the ferroelectric perovskite (Na$_{0.5}$Bi$_{0.5}$)$_{1-x}$Ba$_x$TiO$_3$ by anelastic and dielectric measurements. *Physical Review B*. 2010;81(14):144124.

25. Kruzina TV, Duda VM, Suchanicz J. Peculiarities of optical behaviour of Na$_{0.5}$Bi$_{0.5}$TiO$_3$ single crystals. *Materials Science and Engineering: B*. 2001;87(1):48-52.

26. Yao J, Yan L, Ge W, Luo L, Li J, Viehland D, et al. Evolution of domain structures in Na$_{1/2}$Bi$_{1/2}$TiO$_3$ single crystals with BaTiO$_3$. *Physical Review B*. 2011;83(5):054107.

27. Swain S, Kar SK, Kumar P. Dielectric, optical, piezoelectric and ferroelectric studies of NBT-BT ceramics near MPB. *Ceramics International*. 2015;41(9 Pt A):10710-10717.

28. Kanuru SR, Baskar K, Dhanasekaran R, Kumar B. Growth of NBT-BT single crystals by flux method and their structural, morphological and electrical characterizations. *Journal of Crystal Growth*. 2016;441:64-70.

29. Badapanda T, Sahoo S, Nayak P. Dielectric, Ferroelectric and Piezoelectric study of BNT-BT solid solutions around the MPB region. *IOP Conference Series: Materials Science and Engineering*. 2017;178:012032.

30. Ma C, Tan X. Phase diagram of unpoled lead-free (1-*x*) Na$_{0.5}$Bi$_{0.5}$TiO$_3$-*x*BaTiO$_3$ ceramics. *Solid State Communications*. 2010;150(33-34):1497-1500.

31. Ma C, Tan X, Dul'kin E, Roth M. Domain structure-dielectric property relationship in lead-free (1-*x*)Na$_{0.5}$Bi$_{0.5}$TiO$_3$-*x*BaTiO$_3$ ceramics. *Journal of Applied Physics*. 2010;108(10):104105.

32. Ma C, Tan X. *In situ* Transmission Electron Microscopy Study on the Phase Transitions in Lead-Free (1-*x*)Na$_{0.5}$Bi$_{0.5}$TiO$_3$-*x*BaTiO$_3$ Ceramics. *Journal of the American Ceramic Society*. 2011;94(11):4040-4044.

33. Dul'kin E, Mojaev E, Roth M, Greicius S, Granzow T. Detection of phase transitions in sodium bismuth titanate-barium titanate single crystals by acoustic emission. *Applied Physics Letters*. 2008;92(1):012904.

34. Boyko VS, Garber RI, Kossevich AM. *Reversible Crystal Plasticity*. New York: American Institute of Physics; 1994.

35. Kalitenko VA, Perga VM, Salivonov IN. Determination of the temperatures of phase transitions in barium and strontium titanates by acoustic emission. *Soviet Physics Solid State*. 1980;22:1067-1068.

36. Shimada S, Katsuda Y, Inagaki M. Phase Transition of KNO$_3$ Monitored by Acoustic Emission Technique and the Healing Effect on the γ → α Transition. *The Journal of Physical Chemistry*. 1993;97(34):8803-8807.

37. Dul'kin EA. Ferroic phase boundaries investigations by the acoustic emission method. *Material Research Innovations*. 1999;2(6):338-340.

38. Prabakar K, Mallikarjun Rao SP. Acoustic Emission During Phase Transition in Soft PZT Ceramics Under an Applied Electric Field. *Ferroelectric Letters Section*. 2005;32(5-6):99-110.

39. Garg R, Rao BN, Senyshyn A, Ranjan A. Long ranged structural modulation in the pre-morphotropic phase boundary cubic-like state of the lead-free piezoelectric Na$_{1/2}$Bi$_{1/2}$TiO$_3$-BaTiO$_3$. *Journal of Applied Physics*. 2013;114(23):234102.

40. Suchanicz J, Kruzina TV. Dielectric properties, thermal expansion and heat capacity of (1-*x*)Na$_{0.5}$Bi$_{0.5}$TiO$_3$-*x*BaTiO$_3$ crystals (x = 0, 0.02, 0.025, 0.0325 and 0.05). *Materials Science and Engineering: B*. 2013;178(13):889-895.

41. Hidaka T, Oka K. Isotope effect on BaTiO$_3$ ferroelectric phase transitions. *Physical Review B*. 1987;35(16):8502-8508.

42. Xue F, Liang L, Gu Y, Takeuchi I, Kalinin SV, Chen LQ. Composition-and pressure-induced ferroelectric to antiferroelectric phase transitions in Sm-doped BiFeO$_3$ system. *Applied Physics Letters*. 2015;106(1):012903.